Engineering Notes

ENGINEERING NOTES are short manuscripts describing new developments or important results of a preliminary nature. These Notes cannot exceed 6 manuscript pages and 3 figures; a page of text may be substituted for a figure and vice versa. After informal review by the editors, they may be published within a few months of the date of receipt. Style requirements are the same as for regular contributions (see inside back cover).

Using Electrical Probes to Measure Ion Velocities in Pyrotechnic Plasmas

D. L. Cohen*
Massachusetts Institute of Technology, Cambridge, Massachusetts

Introduction

THERE have been several documented cases of rocket motors, while they were in operation, affecting the local electrical environment on board spacecraft.[1] These electrical perturbations are almost certainly the result of the formation and ejection of charged ions. Significant spacecraft contamination also may occur when positive ions from the rocket's exhaust collect on negatively charged spacecraft surfaces.[2] Any attempt to model these effects requires knowledge of the ion velocity and density distribution inside the rocket motor's pyrotechnic exhaust plume. When pyrotechnic exhaust plumes are simulated in the laboratory, the fluctuating intensity of the burning pyrotechnic will cause many large fluctuations in the plasma parameters of the weakly ionized exhaust, making reliable measurements extremely difficult. Under these conditions, an old standby of plasma physics—the electrical probe—can be used to provide a surprisingly reliable determination of the average ion velocity inside the pyrotechnic exhaust plume.[3]

Experimental Data

The basic experimental setup is shown in Fig. 1. A pyrotechnic plasma is generated inside a combustion chamber using the zirconium, cesium nitrate chemical reaction shown below.

$$3\ Zr + 2\ CsNO_3 \rightarrow 3\ ZrO_2 + 2\ Cs + N_2$$

This reaction has a combustion temperature of 3300 K and, in any given burn, we expect several percent of the cesium atoms (ionization energy of 3.9 eV) to have lost their valence electrons. These Cs^+ ions travel upward and impinge on two cylindrical Langmuir probes held at a bias voltage of -3 V with respect to the combustion chamber. There are no magnetic fields present, and the ambient pressure outside the combustion chamber is 0.05–0.1 Torr. The negative voltage bias ensures that only the Cs^+ ions hit the probes' conducting surfaces—absorbing conduction electrons and generating milliamp-sized currents inside the probe circuitry. This current typically varies on a time scale of 10–100 μs during a burn. The basic cause of the fluctuations is not known, although it does appear to be associated with an intrinsic variability in the rate of chemical reaction rather than peculiarities in the construction of the combustion chamber. The varying chemical reaction produces varying amounts of Cs^+ ions; consequently, the ions in the exhaust plume outside the combustion chamber travel upward in clumps rather than as a smooth distribution. As each ion clump passes a probe, it generates a temporary surge in the probe current. We can use the cross correlations of the random fluctuations in the upper and lower probe currents to determine an average lag time. Since the lower probe is 4 cm closer to the combustion chamber than the upper probe, 4 cm over the lag time will provide a direct measure of the average cesium ion velocity inside the pyrotechnic exhaust plume.

The current from the lower probe is labeled signal A and the current from the upper probe is labeled signal B. During three separate burns a transient waveform analyzer was used to record four separate data sets of 15,000 data points apiece from signals A and B. The signals were sampled at 1-μs intervals, and each data set recorded both signals' peaks and valleys over a 15-ms interval.

We define A_i and B_i to be the sample value (on a scale of 0–255) of signals A and B taken at a time $i\Delta t$ from the start of a given data set (where $\Delta t = 1\ \mu$s). For each data set we define a cross-covariance function C_j such that

$$C_j = \frac{1}{N - |j| - 1} \sum_{i=j}^{N-1} (A_{i-j} - \langle A \rangle) \times (B_i - \langle B \rangle), \quad \text{for } j \geq 0$$

$$C_j = \frac{1}{N - |j| - 1} \sum_{i=0}^{N-|j|-1} (A_{i+|j|} - \langle A \rangle) \times (B_i - \langle B \rangle), \quad \text{for } j < 0 \tag{1}$$

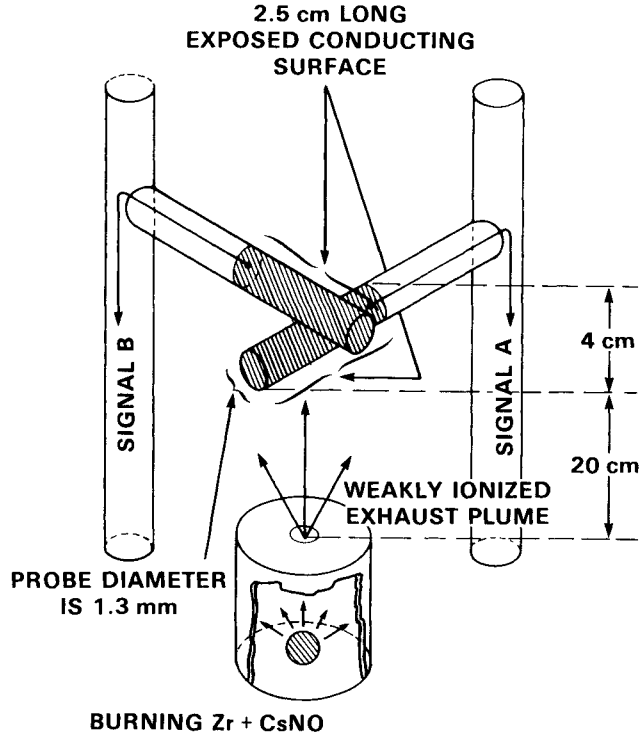

Fig. 1 Experimental setup.

Received Dec. 16, 1987; revision received March 10, 1988.

*Staff Member, Group 95, Countermeasures Technology, Lincoln Laboratory.

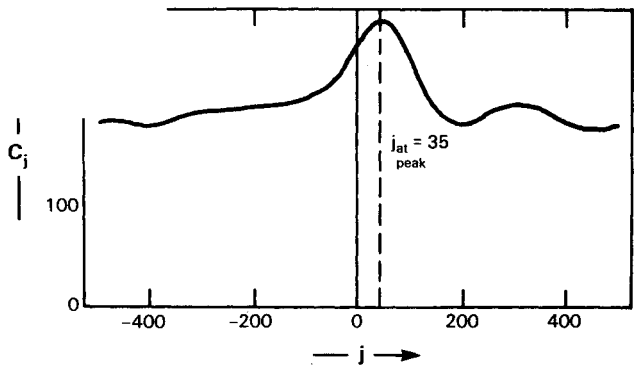

Fig. 2 Cross-covariance function from data set 3.

Table 1 Average lag times and ion velocities from four data sets of 15,000 data points each

Data Set	Average lag time, μs	Average ion velocity, m/s
1	37	1081
2	52	769
3	35	1143
4	25	1600
Average value ± standard deviation	37 ± 10	1148 ± 343

where

$$N = 15{,}000$$

$$j = -450, -449, \ldots, -1, 0, 1, \ldots, 449, 450$$

$$\langle A \rangle = \frac{1}{N} \sum_{i=0}^{N-1} A_i$$

$$\langle B \rangle = \frac{1}{N} \sum_{i=0}^{N-1} B_i$$

Figure 2 is a graph of C_j vs j for the cross-covariance funtion from data set 3. Note that there is a well-defined peak at $j = 35$, which corresponds to an average lag time of 35 μs. Table 1 shows the average lag time, average ion velocity, and associated standard deviations of the cross-covariance functions from all four data sets.

Analysis

Consider a distribution of ions moving one-dimensionally along the x axis of a coordinate system such that $g(v)\,dv$ is the probability of an ion selected at random having a velocity between v and $v + dv$. We then define $N(x,t)\,dx$ to be the number of ions located between x and $x + dx$ at some time $t \geq 0$. The lower probe, which generates signal A, is located at $x = 0$; the upper probe, which generates signal B, is at $x = x_0$. At $t = 0$ a Gaussian-shaped ion clump of standard deviation σ is centered about the lower probe.

$$N(x,0) = N_0 e^{-(x^2/2\sigma^2)} \tag{2}$$

where N_0 is an undetermined constant with units of ions per unit distance. Clearly the current generated in the upper probe at some time $t > 0$ will be proportional to

$$N(x_0,t) = \int_0^\infty N(x_0 - vt,0)g(v)\,dv \tag{3}$$

Assuming that the ion velocity distribution inside the combustion chamber is reasonably close to statistical equilibrium and, thus, Maxwellian in nature, we can approximate the exhaust plume as a molecular beam and set[4]

$$g(v) = (4v^2/\sqrt{\pi}\alpha^3)e^{-v^2/\alpha^2} \tag{4}$$

where

$\alpha = (2kT_c/m)^{1/2}$, $= 640$ m/s

k = Boltzmann constant, $= 1.38 \times 10^{-23}$ j/K

m = mass of cesium ion, $= 2.2 \times 10^{-25}$ kg

T_c = combustion temperature of zirconium cesium nitrate, $= 3300$ K

The value of $\alpha = 640$ m/s determines the velocity scale of the ions; since the current fluctuations occur on a time scale of 10–100 μs, we conclude that the σ values of typical ion clumps will lie between $\sigma = 6.4$ and 0.64 cm. Substituting Eq. (4) into Eq. (3) and integrating gives

$$N(x_0,t) = \frac{4N_0}{\alpha^3 B^3} e^{-(x_0^2/2\sigma^2)} [A/(2\sqrt{\pi}) + \tfrac{1}{2}e^{A^2}(1 + \mathrm{erf}A) \times (A^2 + \tfrac{1}{2})] \tag{5}$$

where

$$B = \sqrt{(1/\alpha^2) + (t^2/2\sigma^2)}$$

$$A = x_0 t/2\sigma^2 B$$

Setting x_0 equal to 4 cm, the distance between the upper and lower probes, we find that $N(x_0,t)$ increases to a maximum as t goes from zero to t_{max} and then drops asymptotically to zero as t gets larger still. When σ is 6.4 cm, $t_{max} = 47$ μs, and, as σ decreases, the value of t_{max} increases to $t_{max} = 48$ μs at $\sigma = 3.6$ cm and $t_{max} = 50$ μs at $\sigma = 0.64$ cm. Clearly the t_{max} values for $\sigma > 3.6$ cm agree with the average lag time of 37 ± 10 μs given by the data in Table 1. However, it is also clear that, for $\sigma < 3.6$ cm, the predicted lag times are several microseconds longer than expected. Given the simple nature of our theoretical model, and the fact that the average lag time is based on only four independent measurements, such a small discrepancy should not be taken too seriously. We can, therefore, tentatively conclude that our ion velocity measurements are in adequate agreement with theoretical expectations.

Conclusion

The operation of rocket motors has been associated with perturbations of the local electrical environment on board spacecraft, and modeling this effect requires knowledge of the average ion velocity inside the motor's pyrotechnic exhaust plume. The fluctuating nature of weakly ionized, pyrotechnic plasmas many times frustrates the traditional methods of plasma physics, making this measurement difficult to perform. However, it is possible to use these fluctuations to advantage instead of regarding them as just another source of experimental error. When two electrical probes are set up inside an exhaust plume so that the ion clumps traveling down the plume impinge on one probe before the other, the average lag time between the two probes' fluctuating currents can be used to measure an average velocity for the ions in the pyrotechnic plasma. The experiment is easy to perform, the data analysis is straightforward, and the final measurements are in agreement with theoretical expectations.

Acknowledgments

The hard work and dedication of Edward Meade in collecting the data used in this paper is warmly and gratefully acknowledged. This work was sponsored by the U.S. Department of the Air Force. The views expressed are those of the author and do not reflect the official policy or position of the U.S. Government.

References

[1]Nanevicz, J. E. and Hilbers, G. R., "Titan Vehicle Electrostatic Environment," Air Force Aeronautical Laboratory, Stanford Research Inst., Menlo Park, CA, AFAL-TR-73-170, July 1973.

[2]Clark, D. M. and Hall, D. F., "Flight Evidence of Spacecraft Surface Contamination Rate Enhancement by Spacecraft Charging Obtained with a Quartz Crystal Microbalance," NASA/Air Force Geophysics Laboratory, NASA CP-2182/AFGL-TR-81-0270, 1981, pp. 493-508.

[3]Schott, L., "Electrical Probes," *Plasma Diagnostics,* edited by W. Lochte-Holtgreven, Wiley, New York, 1968, pp. 668-731.

[4]Ramsey, N. F., *Molecular Beams,* Oxford Univ. Press, London, 1956, p. 20.

Effect of Geometric and Material Nonlinearities on the Propellant Grains Stress Analysis

M. K. Jana,* K. Renganathan,†
and
G. Venkateswara Rao*
Vikram Sarabhai Space Center, Trivandrum, India

Nomenclature

a = inner radius
$[B]$ = matrix relating strains and nodal displacements
b = outer radius
$[D(\bar{\sigma})]$ = elasticity matrix
E_c = Young's modulus for metallic casing
E_1, E_2 = Young's moduli for FRP casing material in axial and hoop directions, respectively
G, G_{12} = shear moduli for propellant and FRP casing, respectively
h = thickness of casing
K = bulk modulus
p = internal pressure
R = radial coordinate
u = radial displacement
w = axial displacement
Z = axial coordinate
ν_c, ν_1, ν_2 = Poisson's ratio for metal and FRP casing, respectively
$\epsilon_z, \epsilon_\theta$ = axial and hoop strains, respectively
$\bar{\sigma}$ = mean normal stress

Received Oct. 16, 1986; revision received Dec. 21, 1987.

*Scientist/Engineer, Structural Engineering Group.
†Programmer, Structural Engineering Group.

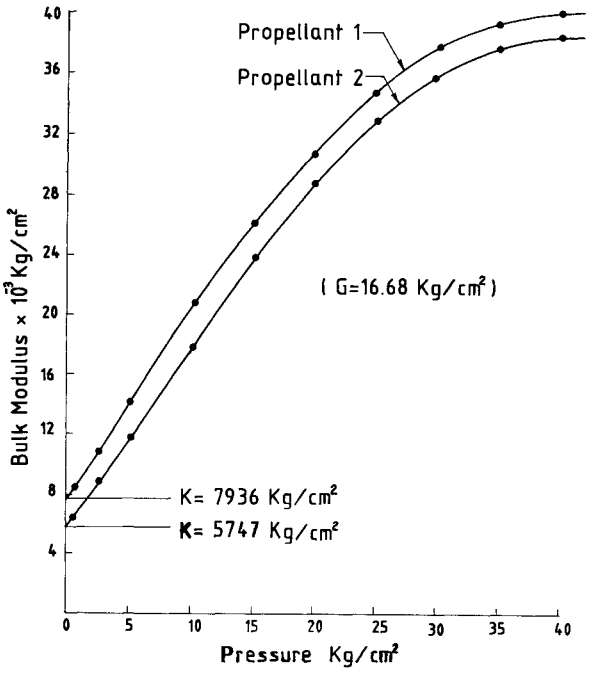

Fig. 1 Variation of bulk modulus with pressure for two HTPB-based propellants.

Introduction

THE presence of porosity or internal voids in solid propellant grain material affects the volumetric response significantly when subjected to pressure load. In a bulk modulus measurement experiment when the propellant specimen is subjected to hydrostatic pressure, the response is highly nonlinear[1] at lower pressure because most of the energy is going into collapsing the internal voids. In this Note, the effect of such material nonlinearity and the geometric nonlinearity on the elastic stress analysis of pressurized propellant grains is studied.

The variation of bulk modulus with hydrostatic pressure obtained from two HTPB-based propellants is shown in Fig. 1. Bulk modulus variation for propellant 1 is used for the analysis of a simple case-bonded cylindrical grain, whereas that for propellant 2 is used for the analysis of an axisymmetric slotted grain. The studies indicate that the effect of material nonlinearity is more predominant as compared to the effect of geometric nonlinearity.

Incremental Finite-Element Analysis

A simple axisymmetric triangular ring element is used to derive element stiffness matrices and load vectors. The effects of geometric and material nonlinearities in the stress analysis have been handled here by the widely used incremental (or step-by-step)[2,3] method. The effect of geometric nonlinearity is incorporated into this formulation by modifying the $[B]$ matrix at each load step, taking into account the change in grain geometry. The nodal forces on the inner surface are modified at each load step considering the expansion of the inner surface. To take into account material nonlinearity, the elasticity matrix

$$[D(\bar{\sigma})] = \begin{bmatrix} K(\bar{\sigma})+\frac{4}{3}G & K(\bar{\sigma})-\frac{2}{3}G & K(\bar{\sigma})-\frac{2}{3}G & 0 \\ & K(\bar{\sigma})+\frac{4}{3}G & K(\bar{\sigma})-\frac{2}{3}G & 0 \\ & & K(\bar{\sigma})+\frac{4}{3}G & 0 \\ \text{(Symmetry)} & & & G \end{bmatrix}$$